International Journal of Pharmaceutics 413 (2011) 220–228

Contents lists available at ScienceDirect

International Journal of Pharmaceutics

journal homepage: www.elsevier.com/locate/ijpharm

Pharmaceutical Nanotechnology

Novel polymeric/lipidic hybrid systems (PLHs) for effective Cidofovir delivery: Preparation, characterization and comparative *in vitro* study with polymeric particles and liposomes

Daniela Belletti[a], Giovanni Riva[b], Giovanni Tosi[a], Flavio Forni[a], Patrizia Barozzi[b], Mario Luppi[b], Maria Angela Vandelli[a], Barbara Ruozi[a,*]

[a] Department of Pharmaceutical Sciences, Via Campi 183, University of Modena and Reggio Emilia, Modena, Italy
[b] Section of Hematology, Department of Oncology, Hematology and Respiratory Diseases, Via del Pozzo, University of Modena and Reggio Emilia, Modena, Italy

ARTICLE INFO

Article history:
Received 14 January 2011
Received in revised form 8 April 2011
Accepted 14 April 2011
Available online 21 April 2011

Keywords:
Polymeric particles (Pps)
Liposomes (Lps)
Polymeric/lipidic hybrid systems (PLHs)
Cidofovir
Cidofovir-loaded liposomes
Controlled release

ABSTRACT

Cidofovir is an antiviral drug active as antitumoral agent a high doses against the Primary Effusion Lymphoma, a herpesvirus HHV8-associated B-cell lymphoma. A novel polymeric/lipidic hybrid system, consisting in a specific combination of biocompatible materials, capable to build a crossbred between polymeric particles and liposomes were prepared and used to stabilize and deliver the drug, unsuccessfully formulated into several types of carriers. This innovative cidofovir-delivering system has structurally been characterized in comparison to multilamellar liposomes and polymeric particles, and then tested for antitumoral efficacy against tumor cells (BCBL-1 cell line). The results demonstrated the improving of drug stability and encapsulation efficiency and suggested that polymeric/lipidic hybrid system could be promising to improve the antitumoral effect of cidofovir even at lower doses.

1. Introduction

Cidofovir, a nucleotide analogue also known as HPMPC, is a broad-spectrum antiviral agent approved by FDA for the treatment of cytomegalovirus retinitis in AIDS patients (De Clercq and Holy, 2005; Gallant and Deresinski, 2003). In addition to the use as antiviral agent, recent studies demonstrated the remarkable antitumour activity of cidofovir in several animal models, associated or not with viral infections (Neyts et al., 1998; Murono et al., 2001; Liekens et al., 1998). Indeed, the antitumour effect of cidofovir has been proposed to be not mediated by the interference with viral cycle, since the drug was able to induce similar levels of apoptosis either in virus-related or unrelated experimental systems (Redondo et al., 2000; Liekens et al., 2001). More recently, cidofovir has also been shown to be an effective treatment against Primary Effusion Lymphoma (PEL), a B cell non-Hodgkin lymphoma involving the serous cavities, invariably associated with Human HerpesVirus-8 (HHV8) and often with Epstein–Barr Virus (EBV) infection. High concentration of cidofovir specifically induced tumor apoptosis against PEL cell lines (Halfdanarson et al., 2006). Moreover, Luppi et al. (2005) demonstrated that intracavity injections of the drug, at higher doses than those required to induce the pro-apoptotic effects *in vitro*, allowed to reach durable remissions (5–15 months) in patients affected by either pleural or peritoneal PEL. A hindrance to the clinical applications of cidofovir is the high systemic toxicity, mainly the nephrotoxicity due to the saturation of the renal transporter hOAT1, which is involved in the elimination of the drug. Furthermore, the chemical properties and the presence of negatively charged phosphonate groups limit the cell uptake of the drug. Cidofovir encapsulation into specific micro- or nanocarriers, able to extend the release of the drug, may represent an effective strategy both to minimize the off-target organ exposure as well as to simultaneously increase the concentration of cidofovir within the site of action. In the last few years, several works described the use of colloidal carrier systems to improve the bioavaibility of cidofovir. Santoyo et al. (2002) proposed PLGA microparticles to improve the topical penetration of the drug. Hillaireau et al. (2006) investigated poly (iso-butylcyanoacrilate) (PIBCA) nanoparticles as carrier to stabilize the drug. These studies showed that the polymeric carriers were hampered by poor encapsulation efficiency, owing to the physical–chemical characteristics of the drug (hydrophilicity, partition coefficient, solubility and pK_a) and to the specific conditions required for particle preparation.

Recently, we proposed to use cationic liposomes to stably encapsulate cidofovir (Ruozi et al., 2010). Unfortunately, the in vivo applicability of such cidofovir carriers is limited by the presence

* Corresponding author. Tel.: +39.059.205.5152; fax: +39.059.205.5131.
E-mail address: barbara.ruozi@unimo.it (B. Ruozi).

0378-5173/$ – see front matter © 2011 Elsevier B.V. All rights reserved.
doi:10.1016/j.ijpharm.2011.04.025

of cationic lipids, inducing a dose-related toxicity. To overcome this problem, in this work we aimed to investigate a novel hybrid system, consisting in a specific combination of biocompatible materials, capable to build a crossbred between polymeric particles and liposomes. This innovative cidofovir-delivering system has structurally been characterized in comparison to multilamellar liposomes and polymeric particles, and then tested for antitumoral efficacy against PEL tumor cells (BCBL-1 cell line).

2. Materials and methods

2.1. Materials

The commercial cidofovir for injection (Vistide®, Gilead Science, Foster City, CA, USA), HPMPC, 1-[(S)-3-hydroxy-2-(phosphonomethoxy)propyl]cytosine dihydrate; $C_8H_{14}N_3O_6P{\cdot}2H_2O$, m.p. 260 °C), was a generous gift of the producer. The product was supplied in clear glass vials each containing 375 mg of anhydrous cidofovir in 5 mL of aqueous solution (75 mg/mL).

L-α-phosphatidylcholine (PC), cholesterol (CHOL) and rhodamine 123 were obtained from Sigma-Aldrich Company (Milan, Italy). Poly(D,L-lactide) (PLA 203H, inherent viscosity in 0.1% $CHCl_3$ at 25 °C = 0.25–0.35 dl/g; Boehringer–Ingelheim, Ingelheim am Rhein, Germany) was used as the polymer. PLA-tetramethylrhodamine conjugate (PLA-Rhod) used to evaluate the internal structure of our carriers was synthesized in our laboratories as previous described (Costantino et al., 2005). PVA (poly vinyl alcohol; 15000 MW) was purchased from Fluka (Milan, Italy). Annexin V-FITC Kit was purchased from Miltenyi Biotec GmbH (Bergisch Gladbach, Germany). RPMI 1640 medium, fetal bovine serum (FBS), and phosphate buffered saline (PBS) were purchased from Euroclone Celbio (Milan, Italy). A Milli-Q water system (Millipore, Bedford, MA, USA), supplied with distilled water, provided high purity water (18 MΩ) for this experiments. All the solvents were of analytical grade; all other chemicals were obtained commercially and used without further purification.

2.2. Methods

2.2.1. Preparation of samples

2.2.1.1. Loaded samples.

2.2.1.1.1. Cidofovir-loaded-polymeric particles (C-Pps). PLA polymeric particles were prepared by W/O/W solvent evaporation method (Bodmeier and Mc Ginity, 1987; Ghaderi et al., 1996; Rosca et al., 2004).

Practically, an appropriate volume of Vistide® containing 12.5 mg of cidofovir (0.16 mL) was removed by the vial and diluted with high purity water to reach 1 mL immediately before the use. The polymer (PLA) (125 mg) was dissolved in 5 mL of dichloromethane (DCM). The aqueous solution was added to the organic one and mixed by sonication (Microson Ultrasonic cell disruptor, Misonix Inc. Farmingdale, NY, USA) (50 W over 1 min) under cooling (5 °C) to obtain a W/O emulsion. This first (inner) emulsion was rapidly added to 15 mL of 1% (w/v) PVA (Poly vinyl alcohol) aqueous solution. The inner W/O emulsion and the PVA aqueous solution were emulsified by ultra-homogenization (Ultraturrax T25, Janke&Kunkel, IKALabortechnik, Staufen, Germany) over 1 min at 13,500 rpm. The resulted W/O/W emulsion was further diluted with 10 mL of PVA 1% (w/v) to have a total external phase of 25 mL of PVA solution and stirred (RW20DZM, Janke&Kunkel, IKA-Labortechnik, Staufen, Germany) at room temperature (1300 rpm for at least 3 h) to allow the solvent evaporation. Polymeric formulation was collected by centrifugation at 10,000 rpm for 10 min at 4 °C (Sorvall RC28S, Dupont, Brussels, Belgium), washed with distilled water and freeze-dried (LyoLab 3000, Heto-Holten, Allerod Denmark, 2 cycles of 24 h).

2.2.1.1.2. Cidofovir-loaded-liposomes (C-Lps). Liposomes were obtained by a modified reverse phase evaporation (REV) method as previously described (Ruozi et al., 2010). Practically, an appropriate volume of Vistide® containing 2 mg of cidofovir (0.027 mL) was removed by the vial and diluted with high purity water to reach 1 mL immediately before the use. Then, 20 mg of lipids (19.04 mg of PC and 0.96 mg of CHOL) were dissolved in 1 mL of chloroform and the cidofovir water solution was gently added. The resulting W/O emulsion was mechanically stirred (RW20DZM, Janke&Kunkel, IKA-Labortechnik, Staufen, Germany) at room temperature (1300 rpm for at least 3 h) to allow the complete solvent evaporation. Then, 4 mL of water were added under agitation to re-suspend liposomes. The un-embedded drug was removed by dialysis (Regenerated Cellulose tubular membrane MWCO 3,500, CelluSep, Membrane Filtration Products, Seguin, TX, USA).

2.2.1.1.3. Cidofovir-loaded-polymeric/lipidic hybrid systems (C-PLHs). The polymeric/lipidic hybrid systems (C-PLHs) were obtained using the same modified REV technique above described for the preparation of C-Lps, but adding PLA (4 mg) to PC and CHOL (20 mg). Really, we tested several compositions in the preparation of PLHs, varying the amount of PLA (2 mg, 4 mg and 6 mg) mixed with 20 mg of lipids. Preliminary tests showed that 6 mg of PLA produced the destabilization of formulation. Moreover, the drug loading was similar to that observed for the liposomes when PLHs were prepared by using less than 3 mg of PLA. Therefore we preferred to use a ratio of 1:5 w/w between PLA and lipid.

2.2.1.2. Unloaded control samples. Unloaded samples (Pps, Lps, PLHs) were prepared using the same experimental conditions above reported, without adding the drug solution.

The composition and the characteristics of the different loaded (C-Pps; C-Lps; C-PLHs) and unloaded (Pps; Lps; PLHs) samples are reported in Table 1. Each sample was prepared in three lots. The samples maintained their stability (in terms of morphology, size, zeta potential, drug loading) when stored at 4 °C and protected from light for 7 days. Then, the formulations were tested within this time.

2.2.2. Characterization of samples

2.2.2.1. Atomic force microscopy (AFM). The morphology of the samples was evaluated by AFM observations performed with an atomic force microscope (Park Instruments, Sunnyvale, CA, USA) at room temperature (about 20–25 °C) operating in air and in non-contact mode. A drop of each sample was diluted with water (about 1:10 v/v) before to be applied on a small mica disk (1 cm × 1 cm); after 2 min, the excess of water was removed using paper filter, then the sample was analyzed.

2.2.2.2. Photon correlation spectroscopy (PCS). Mean particle size and polydispersivity index (PDI) of the samples were determined at 25 °C by PCS using a Zetasizer Nano ZS (Malvern, UK; Laser 4 mW He–Ne, 633 nm, Laser attenuator Automatic, transmission 100–0.0003%, Detector Avalanche photodiode, Q.E. > 50% at 633 nm, T = 25 °C). The results were expressed also as intensity distribution, i.e. the size below which is placed the 10% [D(10)], 50% [D(50)] and 90% [D(90)] of all the particles. The zeta potential was measured using the same equipment with a combination of laser Doppler velocimetry and phase analysis light scattering (PALS). All the data are expressed as means of at least three determinations carried out for each preparation lot (three lots for each sample).

2.2.2.3. Thermal analysis (differential scanning calorimetry; DSC). DSC experiments were carried out to evaluate the possible interaction between the PLA and the lipids and define both the internal

Table 1
Physico-chemical properties and technological characterization of the samples.

Samples	Composition [molar ratio]	Size distribution[a] (nm) (±S.D.)			Zeta potential[a] (mV) (±S.D.)	Encapsulation efficiency[b] [E.E.] (%) (±S.D.)	Drug content[c] (%)
		D(10)	D(50)	D(90)			
Pps	PLA	208.0 (12)	634.5 (54)	1585 (148)	−2.9 (3.2)		
C-Pps		231.5 (5)	619.0 (33)	1625 (174)	−4.0 (2.9)	2.5 (0.9)	0.24
Lps	PC:CHOL 1:0.1	89.5 (6)	430 (42)	2752.5 (580)	−11.0 (3.7)		
C-Lps		155.0 (48)	488.5 (174)	3550.1 (459)	−6.2 (4.4)	11.9 (1.1)	1.17
PLHs	PC:CHOL:PLA	126.7 (24)	567.7 (108)	5183 (497)	4.8 (1.4)		
C-PLHs	1:0.1:0.01	105 (36)	836.2 (268)	5167.5 (334)	7.4 (3.9)	23.0 (0.3)	2.05

[a]Values are mean ± S.D. ($n = 9$).
[b]The percentage of encapsulation efficiency was determined as the ratio of the encapsulated out of the total (encapsulated + free) drug per cent (%). Values are mean ± S.D. ($n = 9$).
[c]The percentage of drug content was expressed as the ratio of the encapsulated drug out of the total mass (encapsulated drug + lipids and/or polymer) per cent. Values are mean ± S.D. ($n = 9$).

structure of PLHs and to evaluate the stability of drug encapsulation into the carriers. DSC curves were recorded on a differential scanning calorimeter equipped with a computerized data station (DSC 200PC "Phox®" Netzsch GmbH, Selb, Germany). Briefly, about 4–5 mg of the samples [Cidofovir, PLA, PC, CHOL, physical mixture between lipids and polymer, lyophilized unloaded carriers (Pps, Lps, PLHs,) and lyophilized cidofovir-loaded carriers (C-Pps, C-Lps, C-PLHs)] were put in crimped aluminium pans (Netzsch) and heated at the heating rate of 2 °C/min from 20 °C to 100 °C and 10 °C/min from 101 °C to 300 °C using dry nitrogen flow (20 mL/min). As the target temperature was reached, the system was cooled by means of liquid nitrogen. Indium (99.99%; Perkin Elmer, Norwalk, USA) (m.p. 156.6 °C; 28.45 ΔH_f J g^{-1}) was used to check the instrument. All experiments were run in triplicate.

2.2.2.4. Hot stage microscopy (HSM analysis-Kofler microscopy). The thermal transition of samples [Cidofovir, PLA, PC, CHOL, physical mixture between lipids and polymer, unloaded carriers (Pps, Lps, PLHs,) and cidofovir-loaded carriers (C-Pps, C-Lps, C-PLHs)] were studied observing their behavior under heating with a Kofler hot stage microscope (Thermovar Reichert, Vienna, Austria) and evaluated using a computer connected photocamera (VC-01, Optika, Brixen, Italy). Practically, the sample was placed on microscope glass slide and dried evacuated under vacuum (10 mmHg) for at least 12 h. The glass slides were placed onto the heating metal block of the microscope and covered with a closed fitting glass plate to prevent heat loss and ensure uniform temperature. The changes were observed under direct and polarized light and simultaneously recorded.

2.2.2.5. Confocal microscopy. CLSM was employed to observe the tetramethylrhodamine distribution within PLHs prepared according the procedure above described, but using a 2% (w/w) of PLA-Rhod respect to the total amount of PLA. In comparison, the structure of liposomes and polymeric particles was evaluated by observing the distribution of rhodamine 123 encapsulated in liposomes and the distribution of tetramethylrhodamine in particles prepared using a 2% (w/w) of PLA-Rhod with regard to the total amount of PLA, as previously described (Ruozi et al., 2011).

CLSM was performed with a Leica DM IRE2 microscope (Mannheim, Germany) and a Leica Confocal System equipped with a scanner multiband 3 channels Leica TCS SP2 with AOBS, laser diode blu COH (405 nm/25 mW), laser Ar (458 nm/5 mW) (476 nm/5 mW) (488 nm/20 mW) (496 nm/5 mW) (514 nm/20 mW), laser He–Ne (543 nm/1.2 mW), laser He–Ne (594 nm) (Orange), laser He–Ne (633 nm/102 mW).

2.2.2.6. Determination of drug loading. The drug loading was expressed as mg of cidofovir encapsulated into 100 mg of formulation (cidofovir and carrier) and as encapsulation efficiency, i.e. the percentage of encapsulated drug related to the initial amount of drug used in the preparation.

The drug loading in the polymeric particles (C-Pps) was determined by a direct methodology. Briefly, 10 mg of particles were dissolved in 2 mL of DCM. Then, 5 mL of water were added to extract the cidofovir and the organic solvent was evaporated at room temperature under stirring (about 60 min). The aqueous solution was filtered (0.2 μm porous filter, Sartorius, Firenze, Italy) to remove the polymer residue and spectrophotometrically analyzed at 273 nm to evaluate the cidofovir concentration.

The drug content of liposomes (C-Lps) and polymeric/lipidic hybrid systems (C-PLHs) was evaluated using an indirect method. Each sample (200 μL) was transferred into a centrifugal ultrafilter device of regenerate cellulose with a 30,000 molecular weight cut-off (Microcon YM-30, Amicon, Vimodrone, Italy) and centrifuged at 10,000 rpm for 15 min (IEC, MiniMax ultracentrifuge, International Equipment Company, Needham Heights, MA, USA). After centrifugation, the ultrafilter device was removed from the centrifuge and the concentration of the un-entrapped drug was measured spectrophotometrically in the surnatant at 273 nm. Cidofovir content in the C-Lps and C-PLHs was calculated as the difference between the total amount of the drug added to the preparation and the amount of un-entrapped drug. All the data are expressed as the means of at least three determinations carried out for each preparation lot.

2.2.2.7. In vitro release studies. A membrane diffusion method was used to evaluate the *in vitro* release studies of cidofovir from C-Pps, C-Lps and C-PLHs. Each sample (1 mL of suspension) was placed in the dialysis tube (CelluSep MWCO 3500, Membrane Filtration Products, Seguin, TX, USA). The dialysis tube (cutoff 3500), permeable to drug alone but not to the particles, was closed at both ends using closure devices (Spectrum Medical Industries, Houston, TX, USA), and placed in 25 mL of distilled water and gently shaken at 100 rpm with a magnetical stirrer in a water bath heated at 37 ± 0.1 °C. The drug diffused out of samples and through the membrane to the receiver phase. At time intervals, a fixed volume (2.5 mL) of the receiving phase was withdrawn and analyzed spectrophotometrically for the drug content. The receiving phase tested was then replaced into the receiving medium to keep constant the dissolution volume. The release study was carried out in triplicate for each sample.

2.2.3. Cell experiments

2.2.3.1. Cell culture. A PEL cell line, namely the HHV8-positive BCBL-1 (immortalized body cavity B-cell lymphoma) cell line, was

cultured in RPMI-1640 medium supplemented with 10% (v/v) of heat-inactivated fetal bovine serum (FBS), L-glutamine 1 mM and antibiotics (complete medium). Cell culture was maintained at 37 °C in a humidified incubator with 5% CO_2 atmosphere.

Before the transfection experiments, density gradient separation procedure was used to isolate and separate viable cells and naturally apoptotic cells. Briefly, the cell suspension was diluted by addition of an equal volume of 0.9% (w/v) NaCl aqueous solution. The dilute suspension was added to a mixture of sodium diatrizoate 9.1% (w/v) and polysaccharide 5.7% (w/v) solution (density 1.007 g/mL and osmolarity 290 mOsm) and centrifuged at 1800 rpm for 25 min at room temperature. After centrifugation, the viable cells formed a distinct band at the sample/solution interface, while apoptotic/dead cells and cell debris were concentrated on the bottom. The viable cells were removed from the interface, twice washed using culture medium and re-seeded. Using this technique, the negative controls showed very low levels of cell death. For all the *in vitro* experiments, a constant concentration of cells (5×10^5 cells/mL) was used.

2.2.3.2. Cytofluorimetric study. To study the toxicity of the cidofovir-delivery systems, different concentrations of empty carriers (unloaded control samples) were added on cells and the results were observed after 4 days. On the basis of our previous work (Ruozi et al., 2010), this time period was identified as the most suitable to evaluate both the toxicity and the activity of drug.

Cell viability was evaluated in triplicate, using Annexin V-FITC Kit (Miltenyi Biotec) and propidium iodide nucleic acid stain (PI, Molecular Probes, Eugene, Or, USA) in order to discriminate apoptotic and dead (necrotic) cells. Apoptotic cells are stained positively for Annexin V-FITC but are negative for staining with PI. Dead cells are stained positively for both Annexin V-FITC and PI, whereas viable cells are negative for both Annexin V-FITC and PI. Briefly, the cells were washed twice, centrifuged at 1000 rpm for 10 min and re-suspended in 50 μL of Annexin V Binding Buffer. Then, 5 μL of FITC (fluorescein isothiocyanate)-conjugated Annexin V solution were added to each cell suspension. After 15 min of incubation in the dark at room temperature, cells were washed twice, centrifuged and re-suspended in Annexin V Binding Buffer. Finally, 10 μL of PI solution were added to this suspension and immediately analyzed by a flow cytometer (FacsCalibur, BD Biosciences, San Jose, CA, USA) equipped with a 15 mW 488 nm air-cooled argon laser. For each cell sample, 20,000 events were collected, then analyzed by CellQuest (BD Biosciences) and Summit softwares (Dako Colorado, Fort Collins, CO, USA).

Once considered the range of system concentrations ensuring a sufficient cell viability, the cells were also treated with cidofovir free or with cidofovir-loaded systems. Also in this case, the analysis was carried out after 4 days and the cytotoxicity of the drug (i.e. cidofovir antitumoral activity) was evaluated at the end of the incubation period by mean of Annexin V-FITC Kit, as above described. Statistical analysis was performed using *t*-test, with the significant level set as $p < 0.05$.

3. Results and discussion

3.1. Characterization of the systems (Pps, Lps and PLHs)

3.1.1. Atomic force microscopy (AFM)

Polymeric particles (Pps) were identified as well-defined vesicles, remaining stable on the mica support for AFM analysis (Fig. 1a). The 3D reconstruction showed a spherical well-defined shape of the Pps, with direct correlation between diameter (width) and height. On the contrary, liposomes obtained with PC and CHOL (Lps) (Fig. 1b) collapsed on the mica surface, showed a flat and heterogeneous structure, and the heights did not correlate with the related diameters. This fact can be due to the interaction between the sample and the substrate, as well as the continuous movement of the tip can induce such a deformation of Lps. However, the vesicle composition plays a key role on the final liposomal structural features (Jass et al., 2000; Ruozi et al., 2005). The hybrid systems (PLHs) were characterized by irregular structures, with a complicated morphology and a rough surface (Fig. 1c). Their aspect on mica support was distorted and remarkable different from that observed either for Pps or Lps.

3.1.2. Photon correlation spectroscopy (PCS)

All the samples were characterized by a heterogeneous population with a variable size distribution (Table 1). Pps and PLHs showed the median diameter D(50) near 600 nm. This value decreased in Lps, being about 430 nm. Moreover, both Pps and Lps showed a negative zeta potential value (−3 mV and −11 mV, respectively). The negative zeta potential value of Pps could be due to the exposition on the Pps surface of carboxylic groups of the PLA molecules, while the negative potential of Lps could be due to the polar head of PC and CHOL in contact with the outer medium. On the contrary, the PLHs showed a slightly positive zeta potential value, probably due to the interaction between PLA and the hydrophilic end of PC, thus covering the reactive anionic groups on the particle surface.

3.1.3. Thermal analysis

To evaluate the structure of the different systems, we studied the thermal behavior. Along with the DSC analysis, the samples were subjected to direct observation by hot stage (Kofler) microscopy during the heating. The comparison of the DSC thermal profile of the samples (Table 2 and Fig. 2) showed remarkable differences amid PLHs, Lps, Pps and the physical mixture obtained mixing PLA and lipids in the same amount used for PLHs preparation. The glass–rubber transition temperature of PLA (at about 50 °C) (Day et al., 2006) was well identified in the thermograms of Pps and physical mixture, while it was absent for PLHs, possibly as a consequence of the strong interaction between polymeric and lipidic components. The decomposition of PC (at about 240 °C) (Ascher and Pershan, 1979; Loomis et al., 1974) was clearly identified in the thermal profiles of physical mixture, Lps as well as PLHs. The fusion temperature of CHOL (at about 150 °C) (Kaloustian et al., 2003) was identified as a broadened transition, quite difficult to be evaluated in both Lps and physical mixture thermograms, while it was not recognized in PLHs, thus demonstrating the different organization of lipids in these structures.

3.1.4. Hot stage (Kofler) microscopy

The direct observation by Kofler microscopy confirmed the hybrid structure of PLHs, made of PLA and lipidic components (Fig. 3), further supporting the interpretation of DSC results. The Lps structure disappeared at the temperature range of 200–250 °C, owing to the decomposition of PC (Fig. 3b). PLA Pps showed the typical glass–rubber transition of the polymer (at about 50 °C), maintaining a well organized and defined structure as the polymer decomposition did not occur in the heating range applied (Fig. 3a). At the microscopical observation, PLHs appeared more similar to Pps than to Lps (Fig. 3c). Although the PLH system composition was based on lipids, the little amount of PLA seemed to be adequate to assure the maintenance of morphological stability.

3.1.5. Confocal microscopy

In order to observe the localization of PLA in PLHs, we substituted the unmodified polymer with PLA covalently marked with the fluorescent probe tetramethylrhodamine (PLA-Rhod). The CLSM analysis (Fig. 4c and d) showed the matrix structure of PLHs. The vesicles appeared characterized by a porous structure, with a wide

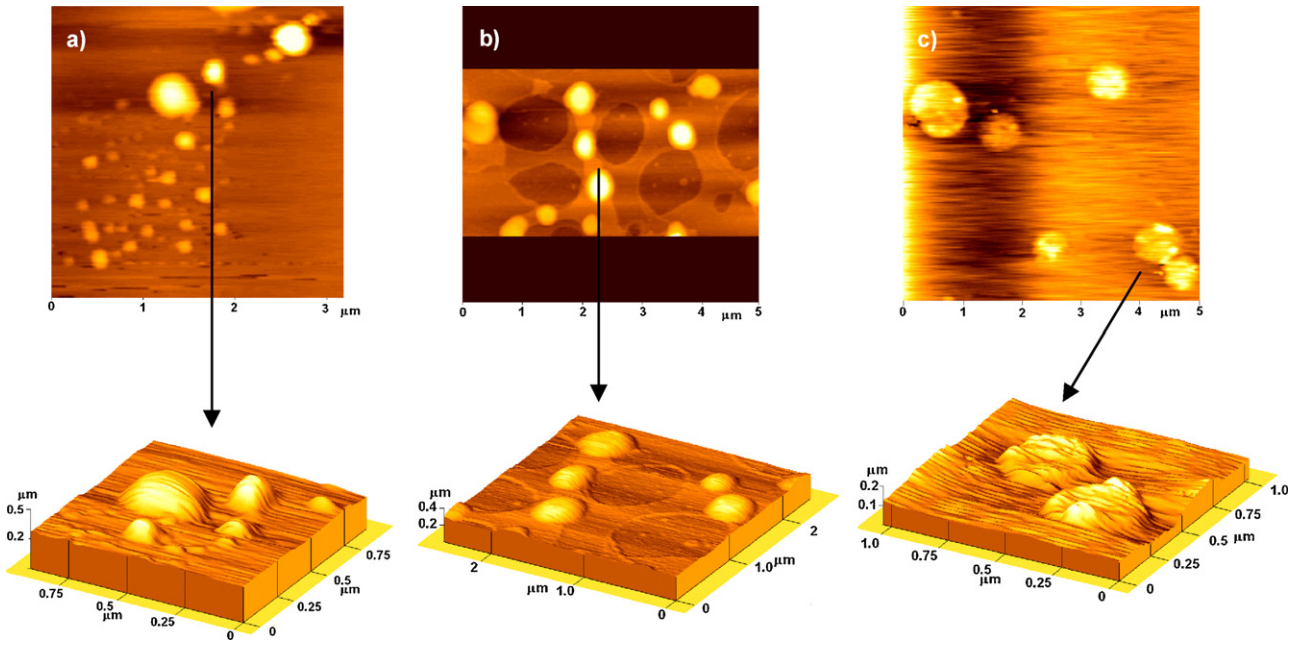

Fig. 1. AFM images of (a) Pps, (b) Lps, (c) PLHs and 3D reconstructions.

Table 2
Thermograms parameters of the based components (PC, CHOL, PLA), cidofovir, physical mixture and the empty (Pps, Lps, PLHs) and drug encapsulated systems (C-Pps, C-Lps, C-PLHs).

Samples	$0^\circ < T > 100^\circ$			$100^\circ < T > 250^\circ$		
	T_{peak}[a] (°C)	T_{onset}[b] (°C)	AH[c] (J g^{-1})	T_{peak}[a] (°C)	T_{onset}[b] (°C)	AH[c] (J g^{-1})
PC				241.0 ± 2.1	240.4 ± 1.1	8.2 ± 0.9
CHOL				150.2 ± 0.2	147.0 ± 0.6	51.9 ± 0.5
PLA	51.1 ± 1.1	48.9 ± 0.8	6.94 ± 0.87			
Cidofovir				269.8 ± 1.2	264.4 ± 4.1	227.1 ± 1.1
Physical Mixture	50.7 ± 0.3	49.1 ± 0.1	1.7 ± 0.21	238.8 ± 0.2	237.6 ± 0.3	2.56 ± 0.4
Pps	47.0 ± 1.1	44.3 ± 0.9	3.5 ± 0.2			
C-Pps	48.8 ± 0.9	45.3 ± 0.3	2.7 ± 0.3			
Lps				238.6 ± 0.2	237.1 ± 0.1	2.9 ± 1.3
C-Lps				232.2 ± 0.8	228.4 ± 2.5	4.4 ± 0.1
PLHs				236.5 ± 1.2	234.7 ± 0.8	3.8 ± 0.9
C-PLHs				229.9 ± 1.3	227.8 ± 0.9	3.9 ± 1.3

[a] T_{peak} was determined as the peak value of the corresponding endothermic phenomena. Values are mean ± S.D. ($n = 3$).
[b] T_{onset} is chosen to identify transition temperature. Values are mean ± S.D. ($n = 3$).
[c] Denaturation enthalpy represent the total area of peak between T_i (initial temperature) and T_f (final temperature). Values are mean ± S.D. ($n = 3$).

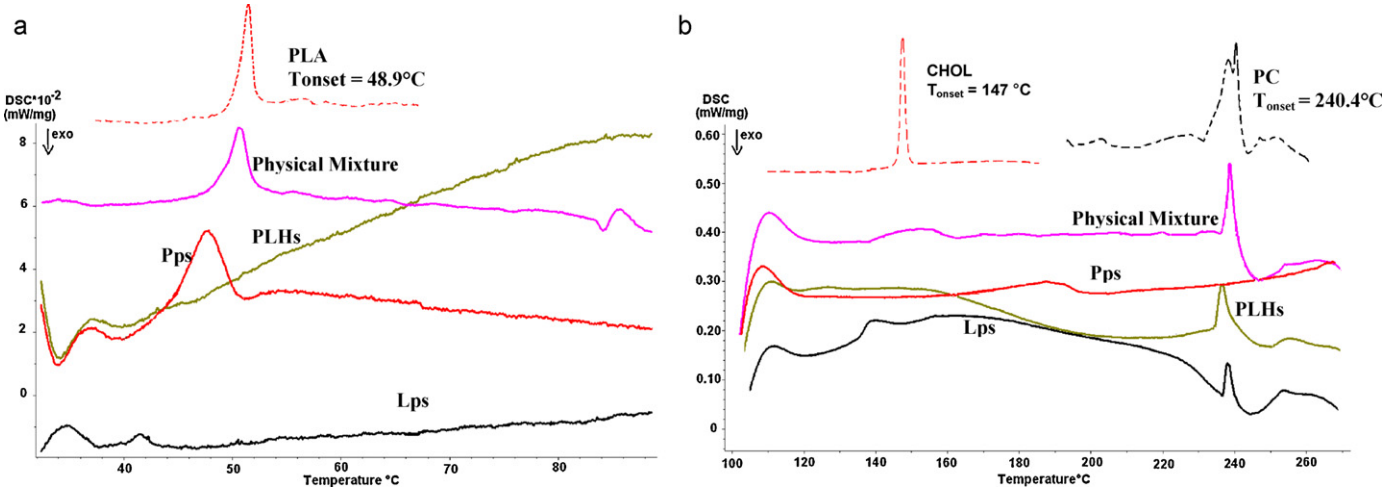

Fig. 2. DSC thermograms of physical mixture, Pps, Lps and PLHs after heating at 2 °C/min (range between 30° and 100 °C-panel (a) and at 10 °C/min (range between 100° and 280 °C-panel (b)). The thermograms have been compared with the transition of the single components of the systems.

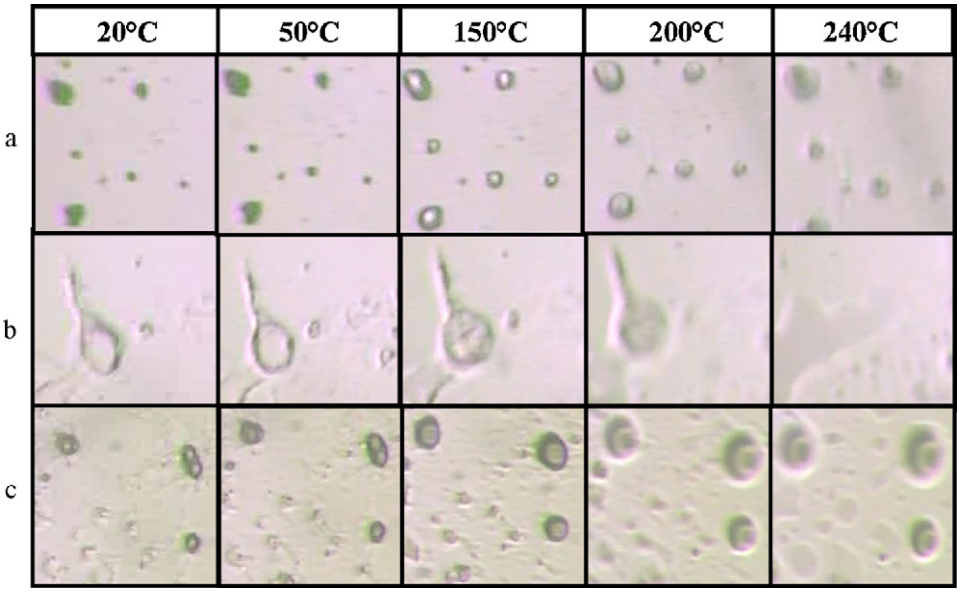

Fig. 3. Hot stage (Kofler) microscopy analysis of (a) Pps, (b) Lps and (c) PLHs. Images were taken at the transition temperature of the related components (glass–rubber transition temperature of PLA ~50 °C; fusion temperature of CHOL ~150 °C; decomposition temperature of PC ~240 °C).

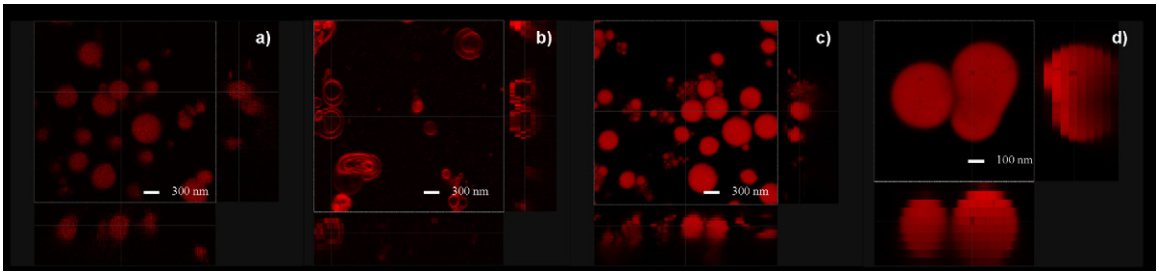

Fig. 4. Confocal images of (a) Pps, (b) Lps and (c) PLHs; (d) magnification of PLHs.

dispersion of PLA-Rhod molecules in the matrix lipidic structure. Therefore, PLHs are almost similar to Pps (Fig. 4a), both formed by very close matrix structure. On the opposite, Lps appeared different as they are formed by multilamellar structure with a close bilayers (colored in red by rhodamine), separating the aqueous inner phase from the outer (Fig. 4b).

3.2. New hybrid systems as cidofovir carriers: characterization, encapsulation and in vitro release studies of cidofovir-loaded PLHs

Cidofovir was encapsulated into polymeric particles (C-Pps), liposomes (C-Lps) and polymeric/lipidic hybrid systems (C-PLHs) as reported in Table 1. The presence of the drug did not affect the size distribution of C-Pps in comparison to the unloaded systems. The increase of both D(50) values and polydispersion of C-Lps and C-PLHs could be an evidence of a certain leaning to increase the diameters of these systems, according to the lipid re-organization during drug encapsulation. The AFM analysis of the samples confirmed the presence of broad size dispersion among the vesicles (data not shown). The zeta potential of all samples was only slightly modified after drug loading, suggesting that only a little amount of drug remained loaded or adsorbed on the vesicle surface.

Although the double emulsion method is the most suitable to obtain a stable encapsulation of hydrophilic drug (Park et al.,

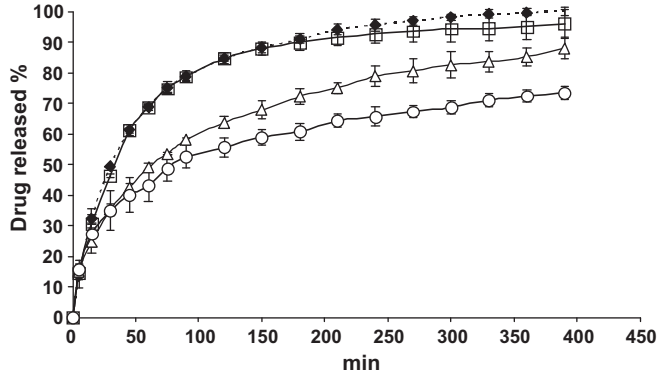

Fig. 5. Diffusion profiles of cidofovir (♦) free and from (○) C-Pps, (□) C-Lps and (△) C-PLHs; influence of carriers composition on the drug release..

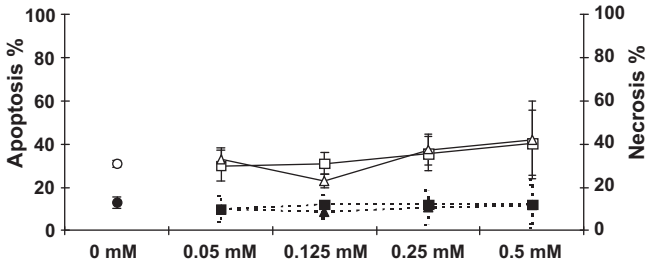

Fig. 6. Cell viability after transfection of different lipid concentrations (*x* axis) of Lps and PLHs. Unbroken line, % of apoptosis after Lps (□) and PLHs (△) transfection; broken line, % of necrosis after Lps (■) and PLHs (▲) transfection. Untreated cells; apoptosis (○) and necrosis (•). Data are expressed as means of three independent experiments ± S.D.

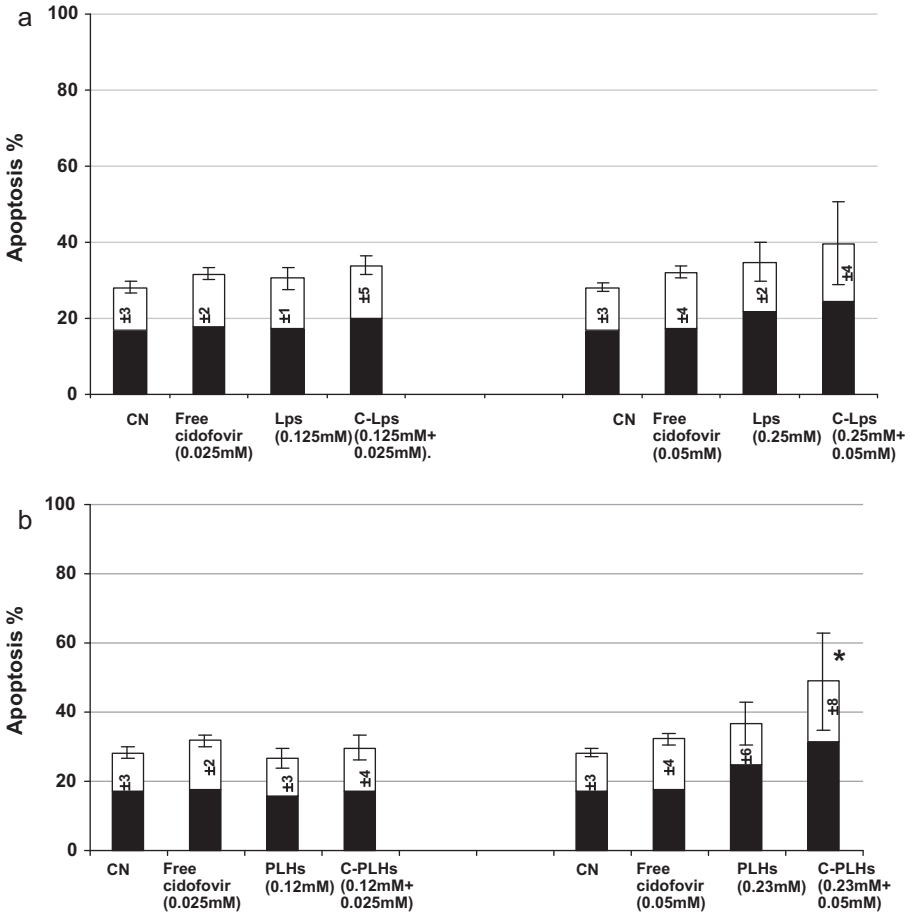

Fig. 7. Cell viability after transfection using C-Lps (Pannel a) and C-PLHs (Pannel b). Histogram bars indicate the percentage of apoptosis; white portions represent the percentage of necrotic cells. Comparison between the percentage of apoptotic cells without treatment (CN), after treatment with free drug, with unloaded carriers and with cidofovir-loaded carriers. Two concentrations of liposome-encapsulated drug (0.025 mM and 0.05 mM) have been tested. Data were expressed ± S.D. (*$p < 0.05$ C-PLHs vs. free cidofovir).

2005), cidofovir was loaded only with low encapsulation efficiency (E.E.) in the C-Pps (E.E. 2.5%). This drawback can be correlated with the amphiphilic structure, which is responsible for the drug tendency to diffuse through the organic phase during C-Pps preparation (Table 1). Instead, in comparison to the C-Pps, the encapsulation efficiency in the C-Lps increased (E.E. 12%), notwithstanding the absence of a positive charge. Indeed, as discussed in ca previous work (Ruozi et al., 2010), the absence of a positive charge in liposomes lowered the amount of loaded cidofovir. However, of note, C-PLHs were able to encapsulate a higher amount of cidofovir (E.E. 23%). Such an enhanced E.E. may be due to the presence of PLA, which is possibly able to stabilize the formulation, decreasing the loss of drug during the preparation procedure.

The interaction between cidofovir and the lipidic component of C-Lps and C-PLHs was demonstrated by the decrease of the PC decomposition temperature observed in DSC analysis (see Table 2). The thermogram of Pps, and particularly the transition temperature of PLA, did not change after cidofovir encapsulation (C-Pps): although this finding could be due to the lack of interaction between the drug and PLA, we are rather in favor of the hypothesis that the absence of any change is due to the little amount of drug incorporated into C-Pps (E.E. about 2.5%).

Moreover, in the systems loaded with cidofovir, the melting of the drug (about 265 °C) could not be observed either by DSC analysis or by hot stage microscopy, suggesting a molecular dispersion of the drug in the matrix structure of the vescicles.

The release curves obtained using the dialysis technique are shown in Fig. 5.

The free drug diffused completely through the membrane into the receiving medium in about 5 h. The diffusion of cidofovir from C-Lps was very similar to that observed for the free drug. Thus, the rapid drug release could be explained by the higher permeability of these systems and the absence of the stable interaction between drug and lipids. The drug diffusion rate from C-Pps was slower (after 5 h, only 70% of drug diffused through the dialysis membrane). This behavior suggested that the low amount of encapsulated drug was strictly incorporated within the polymer chain forming the matrix structure. The presence of PLA in our novel lipid-based delivery systems (C-PLHs) remarkably decreased cidofovir diffusion rate in comparison with C-Lps, particularly during the first 3 h. At this time, only the 70% of drug was released from C-PLHs, in comparison to the 90% diffused from C-Lps.

3.3. *In vitro toxicity of PLHs*

Concerning to the analysis of drug delivery systems, it is pivotal to evaluate the toxicity of the systems in relation to the encapsulation efficiency, which is required to transport an effective amount of drug into target cells (Maurer-Jones et al., 2009). Preliminary experiments were carried out to evaluate the antitumor effect of free cidofovir against BCBL-1 PEL cell line. By assessing the levels of tumor apoptosis and necrosis using flow cytometry, we demonstrated that free cidofovir produced both a

dose-dependent apoptosis and necrosis, well evidenced at 4 and 7 days after transfection (Ruozi et al., 2010). However, only the highest concentrations of free cidofovir ($\geq$ 0.025 mM) induced a massive tumor cell apoptosis in BCBL-1 cell line (data not shown). These data were important to define the minimal drug concentration necessary to induce the cytolytic effect on PEL tumor cells.

Then, different concentrations of unloaded PLHs and Lps were incubated with BCBL-1 cells. The levels of tumor apoptosis and necrosis were assessed 4 days after transfection (Fig. 6); in detail, unbroken lines describe the percentages of apoptotic cells (i.e. dyeing cells), while broken lines describe the percentages of necrotic cells (i.e. dead cells).

Compared with controls (untreated samples; 0 mM of lipids), BCBL-1 cells appeared undamaged after treatment either with Lps or with PLHs, characterized by a lipid range between 0.05 mM and 0.25 mM. Thus, the physiologic lipids, such as PC and CHOL, as well as the PLA used at low doses, seemed to preserve the cellular viability. However, in the presence of lipid concentrations exceeding 0.25 mM, the toxicity results appeared poorly reproducible (i.e. high values of S.D.), possibly as a result of the high amount of preparations added on cells. Thus, the transfection operative conditions and related procedures limited the concentration of Lps and PLHs suitable for transfection experiments.

3.4. *In vitro antineoplastic activity induced by cidofovir-loaded PLHs*

Using the highest tolerated concentrations of carriers (Fig. 6), the ability to effectively deliver cidofovir into BCBL-1 cell line was evaluated by assessing the modification of cell apoptosis/necrosis levels after treatment with C-PLHs compared with C-Lps. We compared the same concentrations of drug encapsulated into C-Lps and C-PLHs (0.025 mM and 0.05 mM); we did not study C-Pps because an un-tolerated amount of Pps would have been needed to achieve the same concentration of active drug as used in C-Lps and C-PLHs. The apoptosis/necrosis data obtained with C-PLHs and C-Lps were also compared to untreated cells (controls), to the treatment with free cidofovir (0.025 mM and 0.05 mM) and to the treatment with unloaded carriers (Lps and PLHs).

Data obtained from the transfection experiments are reported in Fig. 7.

Notwithstanding the wide S.D., the treatment with 0.05 mM cidofovir delivered by C-Lps seemed to improve the pro-apoptotic and pro-necrotic activity, in comparison to free drug (Fig. 7a). Also the new PLHs appeared to be able to both stabilize and transfer the drug into the tumor cells, particularly when a transfection with 0.05 mM cidofovir was operated. As emphasized by the histograms, the concentration of PLHs (0.23 mM of lipids) was well tolerated and induced the same level of apoptosis as observed after Lps treatment. Moreover, the percentage of apoptotic cells after C-PLHs transfection was significantly higher than free cidofovir one (Fig. 7b).

4. Conclusion

Notwithstanding poor results reported in the literature about the effective encapsulation of hydrophilic nucleotide analogues such as cidofovir into liposomal and polymeric particle systems, the new PLHs show improved drug encapsulation efficiencies and stabilization (up to 10 times respect to polymeric particles and twice than conventional lipidic systems). Moreover, our data suggest that the higher amount of drug encapsulated and delivered by C-PLHs (E.E. 23%) may produce a moderate but detectable increase in the antitumor activity of cidofovir if compared with the action operated by C-Lps, as demonstrated by the percentage of apoptotic/necrotic cells (more than 50% after C-PLHs treatment and less than 40% after C-Lps treatment). Importantly, a significant difference was observed between the antitumor activity mediated by C-PLHs and that exerted by free drug.

With regards to other lipidic or polymeric carriers, PLHs consistently showed the liposomal versatility and ability to fuse and deliver the drug into the cells, in association with the structural advantages of the polymeric internal matrix, strikingly improving their stability and encapsulation efficiency. The size and the polydispersity suggest that PLHs could be proposed for intrapleuric/intracavity administration; the efficient local delivery operated by our systems should reasonably enhance the intratumoral accumulation of the drug both improving the therapeutic efficiency and reducing the systemic toxicity. These structural and functional features of novel cidofovir-loaded PLHs may eventually also explain the promising improvement of the antitumoral effect even at lower cidofovir doses.

Acknowledgements

Authors are grateful to Gilead Science for the generous gift of Vistide®. Thanks are also due to Centro Interdipartimentale Grandi Strumenti (CIGS) of the University of Modena e Reggio Emilia and particularly to Dr. Tombesi Andrea for his assistance in the confocal image acquisitions.

References

Ascher, S.A., Pershan, P.S., 1979. Aligment and defect structures in oriented phosphatidylcholine multilayers. Biophys. J. 27, 393–422.
Bodmeier, R., Mc Ginity, R.W., 1987. The preparation and evaluation of drug-containing poly(DL-lactide) microspheres formed by the solvent evaporation method. Pharm. Res. 4, 465–471.
Costantino, L., Gandolfi, F., Tosi, G., Rivasi, F., Vandelli, M.A., Forni, F., 2005. Peptide-derivatized biodegradable nanoparticles able to cross the blood–brain barrier. J. Control Release 108, 84–96.
Day, M., Nawaby, A.V., Lia, X., 2006. A DSC study of the cristallization behaviour of polylactic acid and its nanocomposites. J. Therm. Anal. Calorim. 86, 623–629.
De Clercq, E., Holy, A., 2005. Acyclic nucleoside phosphonates: a key class of antiviral drugs. Nat. Rev. Drug Discov. 4, 928–940.
Gallant, J.E., Deresinski, S., 2003. Tenofovir Disoproxil Fumarate. Clin. Infect. Dis. 37, 944–950.
Ghaderi, R., Sturesson, C., Carlfors, J., 1996. Effect of preparative parameters on the characteristics of poly(D, L-lactide-co-glycolide) microspheres made by the double emulsion method. Int. J. Pharm. 141, 205–216.
Halfdanarson, T.R., Markovic, S.N., Kalokhe, U., Luppi, M., 2006. A non-chemotherapy treatment of a primary effusion lymphoma: durable remission after intracavitary cidofovir in HIV negative PEL refractory to chemotherapy. Ann. Oncol. 17, 1849–1850.
Hillaireau, H., Le Doan, T., Besnard, M., Chacun, H., Janin, J., Couvreur, P., 2006. Encapsulation of antiviral nucleotide analogues azidothymidine-triphosphate and cidofovir in poly(iso-butylcyanoacrylate) nanocapsules. Int. J. Pharm. 324, 37–42.
Jass, J., Tjärnhage, T., Puu, G., 2000. From liposomes to supported, planar bilayer structures on hydrophilic and hydrophobic surfaces: An atomic force microscopy study. Biophys. J. 79, 3153–3163.
Kaloustian, J., Pauli, A.M., Lechene de la Porte, P., Lafont, H., Portugal, H., 2003. Thermal analysis of anhydrous and hydrated cholesterol. J. Therm. Anal. Calorim. 71, 341–351.
Liekens, S., Andrei, G., Vandeputte, M., De Clercq, E., Neyts, J., 1998. Potent inhibition of hemangioma formation in rats by the acyclic nucleoside phosphonate analogue cidofovir. Cancer Res. 58, 2562–2567.
Liekens, S., Neyts, J., De Clercq, E., Verbeken, E., Ribatti, D., Presta, M., 2001. Inhibition of fibroblast growth factor-2-induced vascular tumor formation by the acyclic nucleoside phosphonate cidofovir. Cancer Res. 61, 5057–5064.
Loomis, C.R., Janiak, M.J., Small, D.M., Shipley, G.G., 1974. The binary phase diagram of lecithin and cholesteryl linolenate. J. Mol. Biol. 86, 309–324.
Luppi, M., Trovato, R., Barozzi, P., Vallisa, D., Rossi, G., Re, A., Ravazzini, L., Potenza, L., Riva, G., Morselli, M., Longo, G., Cavanna, L., Roncaglia, R., Torelli, G., 2005. Treatment of herpesvirus associated primary effusion lymphoma with intracavity cidofovir. Leukemia 19, 473–476.
Maurer-Jones, M.A., Bantz, K.C., Love, S.A., Marquis, B.J., Haynes, C.L., 2009. Toxicity of therapeutic nanoparticles. Nanomedicine 4, 219–241.
Murono, S., Raab-Traub, N., Pagano, J.S., 2001. Prevention and inhibition of nasopharyngeal carcinoma growth by antiviral phosphonated nucleoside analogs. Cancer Res. 61, 7875–7877.
Neyts, J., Sadler, R., De Clercq, E., Raab-Traub, N., Pagano, J.S., 1998. The antiviral agent cidofovir [(S)-1-(3- hydroxy-2-phosphonylmethoxypropyl)cytosine] has pronounced activity against nasopharyngeal carcinoma grown in nude mice. Cancer Res. 58, 384–388.

Park, J., Ye, M., Park, K., 2005. Biodegradable polymers for microencapsulation of drugs. Molecules 10, 146–161.
Redondo, P., Idoate, M., Galofrè, J.C., Solano, T., 2000. Cidofovir inhibits of B16 melanoma cells in vivo. Br. J. Dermatol. 143, 741–748.
Rosca, I.D., Watari, F., Uo, M., 2004. Microparticle formation and its mechanism in single and double emulsion solvent evaporation. J. Control Release 99, 271–280.
Ruozi, B., Belletti, D., Tombesi, A., Tosi, G., Bondioli, L., Forni, F., Vandelli, M.A., 2011. AFM, ESEM, TEM and CLSM in liposomal characterization: a comparative study. Int J Nanomedicine. 6, 557-563.
Ruozi, B., Riva, G., Belletti, D., Tosi, G., Forni, F., Mucci, A., Luppi, M., Barozzi, P., Vandelli, M.A., 2010. Cidofovir as anticancer drug: liposomal formulation and in vitro study. Eur. J. Pharm. Sci. 41, 254–264.
Ruozi, B., Tosi, G., Forni, F., Fresta, M., Vandelli, M.A., 2005. Atomic force microscopy and photon correlation spectroscopy: Two techniques for rapid characterization of liposomes. Eur. J. Pharm. Sci. 25, 81–89.
Santoyo, S., Ga de Jalon, E., Ygartua, P., Renedo, M.J., Blanco-Prieto, M.J., 2002. Optimization of topical cidofovir penetration using microparticles. Int. J. Pharm. 242, 107–113.